# An approach to OCT-based microvascular imaging using reference-free processing of complex-valued B-scans

Lev A. Matveev[1,2,3*], Grigory V. Gelikonov[1,2], Alexandr L. Matveyev[1,2], Alexander A. Moiseev[1], Sergey Ksenofontov[1], Valentin M. Gelikonov[1,2,3], Marina A. Sirotkina[2], Natalia L. Buyanova[2], Natalia D. Gladkova[2], Valentin Demidov[4], Alex Vitkin[2,4], and Vladimir Yu. Zaitsev[1,2,3]

[1]Institute of Applied Physics Russian Academy of Sciences, Ulyanova Street 46, 603950 Nizhniy Novgorod, Russia
[2]Nizhny Novgorod State Medical Academy, Minin Square 10/1, 603005 Nizhny Novgorod, Russia
[3]Nizhny Novgorod State University, Gagarina Avenue 23, Nizhny Novgorod 603950, Russia
[4]University of Toronto and University Health Network, 610 University Ave., Toronto, Ontario, M5G 2M9, Canada

## ABSTRACT

We describe a modification of a recently proposed unconventional OCT approach to 3D microvasculature imaging based on high-pass filtering of B-scans in the lateral direction. The B-scans are acquired in M-mode-like regime with highly overlapped A-scans. The goal of the described modification is to suppress non-fluid artifacts in the resultant microcirculation images. The modification is based on the amplitude normalization procedure of complex-valued OCT signal before subsequent processing. This allows one to efficiently suppress imaging degradation due to the influence of very bright spots/lines (e.g. from hairs on the surface) and retain images of real flows inside the tissue without any artificial cut-off of the surface signal, or application of pixel-intensity thresholds, or signal classification approaches.

**Keywords:** optical coherence tomography, angiography, image processing, speckle variance, flow diagnostics

## 1. INTRODUCTION

Ways of utilization of speckle-structure variability of OCT images attracts significant attention in the context of elastographic (see, e.g., ref.[1] and reviews[2,3]) and especially angiographic imaging (see, e.g. ref.[4] and reviews[5,6]). In elastographic problems, the motion of scatterers produced by the tissue deformation can be used for visualizing differences in the strain level, whereas for microvasculature visualization, the natural motion of scatterers in the blood due to both regular flow and Brownian motion of blood particles can be used as a contrast mechanism in order to single out "liquid" pixels corresponding to blood-filled microvessels from the surrounding "solid" tissue. In some cases the Brownian motion can even give strongly dominating contribution to the speckle-texture variability[7]. The latter fact ensures better sensitivity of the speckle-contrast methods compared to phase-resolved (Doppler) methods that demonstrate strongly decreased sensitivity to flows with low velocity in the axial direction of the optical beam[5]. On the other hand, despite usually better sensitivity of the speckle-contrast methods, the conventionally discussed forms of such methods do not retain quantitative information about the flows in the visualized network of microvessels.

For mapping regions of increased speckle-texture variability, various particular methods can be used, including correlation processing[4] and speckle-variance (Sv) methods[5,6,7]. The common feature of these approaches is that they use comparison of entire B-scans obtained consequently in the same plane. The time of acquisition of individual A-lines typically is 2-3 orders of magnitude smaller than the interval between B-scans, which usually amounts to tens of milliseconds. Thus obtaining of several consequent sufficiently-well coincided B-scans in order to reliably distinguish stabler "solid" pixels and faster decorrelating "liquid" pixels is significantly complicated by inevitable bulk motions of living tissue. For example, usually in realizations of the Sv approach, the typical decorrelation times for the blood in vessels on the order $10^1$-$10^2$ μs require obtaining 8-10 repeated B-scans in a stack. However, with increasing time between compared B-scans the processing becomes also stronger sensitive to low-frequency tissue motions (breathing, heart beating, etc.)[8]. Thus realization of the conventionally discussed speckle-contrast methods of microvascular imaging

Optical Coherence Imaging Techniques and Imaging in Scattering Media, edited by Brett E. Bouma, Maciej Wojtkowski, Proc. of SPIE-OSA Biomedical Optics, SPIE Vol. 9541, 954106 · © 2015 SPIE-OSA · CCC code: 1605-7422/15/$18 · doi: 10.1117/12.2184937

is complicated by the necessity of stabilization of the inspected tissue and/or elimination of the clatter-motion artifacts in the image post-processing. This stabilization is favorable for increasing the contrast between the microvessles and the surrounding tissue, but in so-obtained images all strongly decorrelated speckles in the vasculature texture look similar and do not retain biologically important information about decorrelation-time differences for different vessels.

Besides the motion artifacts, one of significant problems is reduction of artifacts from motionless background especially from the surface[9]. Several signal processing techniques were developed in the recent years to reduce the contributions of those artifacts to the total microvasculature images. For example, some algorithms based on the elimination from processing the points that overcome somehow defined (pre-selected or adaptive) intensity threshold; other algorithms are intended to detect the surface and cut it off; and another class of algorithms analyze the signal structure (e.g. histograms) and perform certain classification to exclude the artifacts[9].

Here, we propose a novel approach to distinguish and subtract saturated signals (e.g. hotspots and hairs on the surface) from the real flows inside the tissue without any artificial cut-off of the surface signal, intensities thresholds or signal classification. We propose the modification of our recently proposed M-mode like OCT approach based of full complex valued signal processing by applying the normalization procedure to the complex signal on its amplitude before further processing.

## 2. M-MODE-LIKE OCT MICROANGIOGRAPHY

Recently we proposed an OCT-based method[10,11] for 3D visualizing blood microcirculation which can be considered as a kind of hybrid technique combining elements of speckle-contrast and phase-resolved methods. The proposed approach uses reference-free processing of individual complex-valued B-scans in which A-scans are densely spaced, so that the horizontal step between the adjacent A-scans is significantly smaller than the optical-beam diameter. This pattern can be viewed as M-mode-like, so that the speckles corresponding to the "solid" tissue (in which scatterers are motionless) look as strongly elongated "dashes" in the lateral direction along the dense B-scan. In contrast, the regions corresponding to cross sections of vessels containing moving scatterers demonstrate significantly higher variability of the speckle pattern in the lateral direction. This statement is illustrated by Fig. 1 showing a fragment of conventional structural image in which the encircled region of "short-dash" speckles corresponding to a vessel cross section is clearly distinct from the speckle structure of the surrounding "solid" tissue. Thus the liquid areas are characterized by increased speckle variability, so that in a broad sense this contrast mechanism can be viewed as specke-contrast one by analogy with correlation mapping and Sv-method, but with an important difference that it manifests itself within the same B-scan and does not require comparison with reference B-scans obtained for the same position.

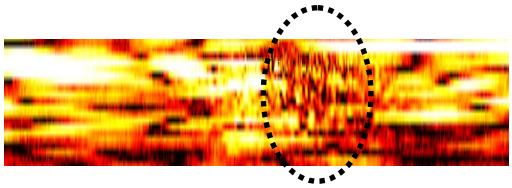

Fig. 1. A small fragment of high-density B-scan illustrating the distinction between the "long-dash" speckles corresponding to the solid tissue with motionless scatterers and "short-dash" speckles corresponding to moving scatterers within a vessel cross section (encircled in the figure). The size of the imaged region is about 70 μm in depth and 120 μm in the lateral direction.

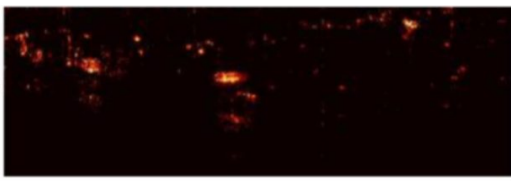

Fig. 2. An example of resultant B-scan after high-pass filtering and downsampling to the natural resolution of the OCT scanner. Only vessel cross sections containing moving scatterers are retained in the image. The size of the imaged region is about 700 μm in depth and 2000 μm in the lateral direction.

Next, the principle of singling out the areas of increased speckle variability in the proposed method is also different from straightforward comparison of neighboring A-scans points. It is clear from Fig. 1 that for the higher-variable "liquid" pixels, the spatial spectrum in the horizontal (lateral) direction is significantly extended towards the high-frequency region. Therefore, applying high-pass filtering to the horizontal spatial spectrum of such an image allows one to predominantly retain the B-scan areas corresponding to cross-sections of the vessels, whereas the contribution of motionless scatterers in the "solid" tissue becomes strongly suppressed. An example of so-obtained image via

high-pass filtering of an initial high-density (oversampled) B-scan and subsequent down-sampling to the natural lateral resolution of the OCT scanner in shown in Fig. 2. After the high-pass filtering procedures, only vessel cross-sections containing moving scatterers are retained in the scan.

Further, by varying the threshold frequency of the high-pass filter, one can retain scatterers with different rates of speckle variability and, correspondingly grade the vessels in terms of the characteristic decorrelation time. A stack of B-scans acquired via the above-described principles ensures obtaining of a 3D image of the microvasculature. Using conventional procedures, one can obtain *en face* images either in the form of maximum-intensity projections (MIP) in the horizontal plane or two-dimensional depth-encoded projections.

For the experimental demonstrations, we used a home-made spectral-domain OCT scanner with the central optical wavelength 1.32 μm, bandwidth of 106 nm and a rate of 20 kHz for spectral fringes (yielding 10 kHz rate of the formed complex-valued A-scans). The axial and lateral resolutions of the system are 10 μm and 20 μm, respectively. In the depth direction, the spectrometer array enables 256 pixels and the chosen number of B-scans for 3D scanning also equals 256. The microvasculature images were obtained using BalbC mice with Colo26 tumor inoculated on its ear.

It can be emphasized that in the experiments there was a motions of the ear due to animal breathing with the characteristic frequency 3-4 Hz. However, comparison of average phases of adjacent A-scans allowed for quite efficient compensation of the phase shifts due to bulk (depth-averaged) tissue motions, whereas the local variations in the speckles' phases and amplitudes were retained. This compensation becomes possible because of the small time gap between the A-scans (0.1 μs), so that the translational displacements of the tissue yet affect only on phase of the complex-valued signal.

## 3. AMPLITUDE-NORMALIZED M-MODE-LIKE OCT.

Here we describe a novel variant of the described above approach[10]. The goal of this modification is to reduce in resulting filtered microvasculature images the contribution from high-intensity points (e.g. signal-saturating points on the surface) that are not related to vessels. For such high-intensity motionless points, the ratio between the two signal quadratures does not vary in time, but due to high amplitude their lateral (along B-scans) spectrum contains relatively high energy that leaks up to its high-frequency part and thus masks contributions of genuine moving scatterers. To suppress the masking influence of such high-intensity points, we perform amplitude normalization of the full complex signal $S(x,y,z)$:

$$\widetilde{S}(x,y,z)=\frac{S(x,y,z)}{\left|S(x,y,z)\right|}=\frac{A(x,y,z)e^{-i\varphi(x,y,z)}}{A(x,y,z)}=e^{-i\varphi(x,y,z)}\ , \tag{1}$$

where the (*x,y,z*) are point coordinates in 3D-data-pack (for example, *x* is the lateral direction in the plane of B-scan, $y$ is the transverse direction and $z$ is the depth); $A(x,y,z)$ is the amplitude of the complex valued signal in the (*x,y,z*) point and $\varphi(x,y,z)$ is the phase of this point. Then we apply the above-described HP filtering to the new normalized signal $\widetilde{S}(x,y,z)$.

Figure 3 shows an example of application of this approach to suppress the hotspots and highly scattering areas on the surface of the mouse skin *in vivo* (ear of the BalbC mouse). Figure 3(a) is the *en face* OCT signal from the surface of the mouse's ear. It clearly shows very bright spots in some areas of the surface. The cause of the high brightness of such areas can be due to the presence of highly reflective objects on the surface, as well as enhanced coupling of the scattered signal with the receiving fiber due better angular correspondence between the fiber and the unevenly inclined surface.

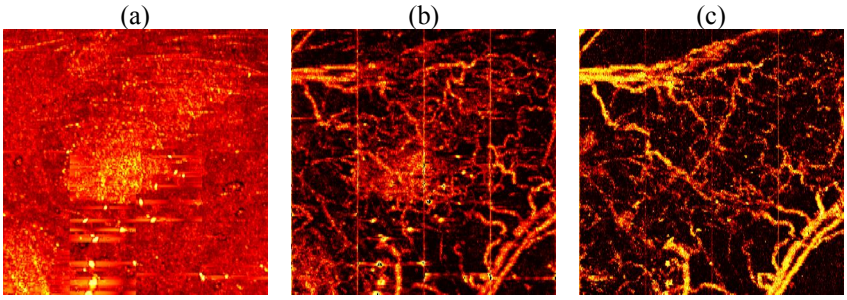


Fig. 3. Demonstration of the efficiency of the proposed normalization for reducing the artifacts arising from hotspot areas on the tissue surface. Panel (a) - *en face* OCT image of mouse's ear surface; panel (b) - *en face* microvasculature maximum-intensity projection (MIP) image obtained by HP filtering of the full complex signal; panel (c) *en face* microvasculature MIP image obtained by filtering of the normalized signal. The MIP's depth range is 600 μm and the chosen threshold frequency of the high-pass filter is 96 Hz. Significant reduction of artifacts related to surface hotspots is clearly seen in panel (c) in comparison with panel (b).

Figure 3(b) is the angiographic image obtained by filtering the full complex signal $S(x, y, z)$ and Figure 3(c) corresponds to the filtered normalized signal $\tilde{S}(x, y, z)$. It is clearly seen is Figure 3(a) the areas with strongly increased signal in the left-bottom and center regions. These bright image features produce artifacts in the microcirculation image shown in Figure 3(b) that is obtained after processing the full (not-normalized) complex-valued signal. The efficiency of the normalization is demonstrated in Figure 3(c) where the microvasculature image is obtained after processing the normalized complex-valued signal. Significant reduction of the influence of hotspot surface artifacts is clearly seen from the comparison between panel (b) and panel (c) of Figure 3.

Similar demonstrations are shown in Figure 4 for the case of a highly haired part of the mouse ear. Hairs that are seen in the surface OCT image (Figure 4(a)) produce a large number of artifacts looking like vessels in the resulting microcirculation image shown in Figure 4(b) that is obtained by processing the full not-normalized complex-valued signal. The normalization of the signal before processing suppresses this hair-induced structure from the microcirculation image as shown in Figure 4(c). The efficiency of the hair-influence suppression is clearly seen here.

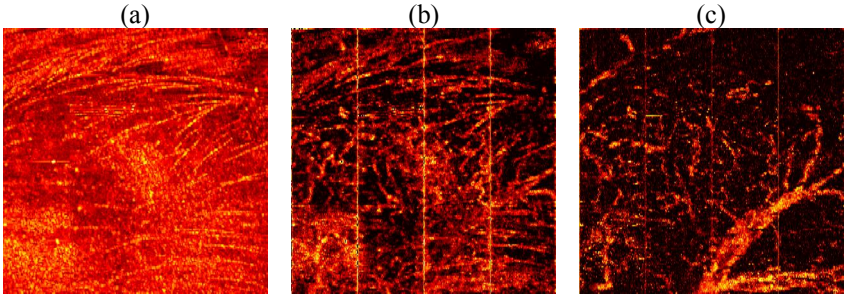


Fig. 4. The demonstration of the efficiency of the proposed normalization for reducing the artifacts arising from the hairs on the tissue surface. Panel (a) - *en face* OCT image of mouse ear surface where brightly scattering hairs are clearly seen; panel (b) is the *en face* microvasculature MIP image obtained by filtering the full complex signal without normalization; panel (c) is the *en face* microvasculature MIP image obtained by filtering of the normalized signal. The MIPs depth range is 600 μm and the chosen threshold frequency of the high-pass filter is 96 Hz. Significant reduction of hair-induced artifacts is clearly seen in from the comparison between panel (b) and panel (c).

## 4. DISCUSSION AND CONCLUSION

The presented examples demonstrate the possibility of the separation and suppression of the artifacts induced by the surface hotspots from the resulting microcirculation images by preliminary application of the normalization procedure to the full complex-valued signal before further processing. This approach allows one to suppress/separate artifacts from bright motionless points from the real flows inside the tissue without any artificial cut-off of the surface signal, application of pixel-intensity thresholds signal classification methods. The proposed approach not only makes it possible to reduce the influence of hotspots on the resulting microvasculature images, but also allows one to exclude from the resulting image such challenging artifacts like hair-induced vessel-like lines as demonstrated in Figure 4. Acknowledgements

The authors acknowledge support of the Russian Federation Government contract No 14.B25.31.0015 for Leading Scientists to Russian Educational Institutions and the Russian Foundation of Basic Research (grant No 15-42-02513). VYZ and VMG acknowledge partial support by the contract No 02.B49.21.0003 between the Russian Ministry of Education and Nizhny Novgorod State University.

## REFERENCES

[1] Zaitsev, V. Yu., Matveev, L. A., Matveyev, A. L., Gelikonov, G. V., and Gelikonov, V. M., "Elastographic mapping in optical coherence tomography using an unconventional approach based on correlation stability," Journal of Biomedical Optics 19(2), 021107 (2014).

[2] Zaitsev, V. Y., Gelikonov, V. M., Matveev, L. A., Gelikonov, G. V., Matveyev, A. L., Shilyagin, P. A., and Vitkin, I. A., "Recent trends in multimodal optical coherence tomography . I . Polarization-sensitive oct and conventional approaches to OCT elastography," Radiophys. Quant. Electron. 57, 52 (2014).

[3] Kennedy, B. F., Kennedy, K. M., and Sampson, D. D., "A review of optical coherence elastography: fundamentals, techniques and prospects," IEEE J. Sel. Topics Quantum Electron. 20, 7101217 (2014).

[4] Jonathan, E., Enfield, J., and Leahy, M. J. "Correlation mapping method for generating microcirculation morphology from optical coherence tomography (OCT) intensity images," Journal of Biophotonics 4(9), 583–587 (2011).

[5] Zaitsev, V. Y., Vitkin, I. A., Matveev, L. A., Gelikonov, V. M., Matveyev, A. L., and Gelikonov, G. V., "Recent Trends in Multimodal Optical Coherence Tomography. II. The Correlation-Stability Approach in OCT Elastography and Methods for Visualization of Microcirculation," Radiophys. Quant. Electron. 57, 210 (2014).

[6] Mahmud, M. S., Cadotte, D. W., Vuong, B., Sun, C., Luk, T. W. H., Mariampillai, A., and Yang, V. X. D., "Review of speckle and phase variance optical coherence tomography to visualize microvascular networks," Journal of Biomedical Optics 18, 050901 (2013).

[7] Mariampillai, A., Standish, B. A., Moriyama, E. H., Khurana, M., Munce, N. R., Leung, M. K. K., Jiang, J., Cable, A., Wilson, B. C., Vitkin, I.A., and Yang, Y. X. D., "Speckle variance detection of microvasculature using swept-source optical coherence tomography," Optics Letters 33, 1530 (2008).

[8] Matveev, L. A., Zaitsev, V. Y., Matveev, A. L., Gelikonov, G. V., Gelikonov, V. M., and Vitkin, A., "Novel methods for elasticity characterization using optical coherence tomography: Brief review and future prospects," Photonics & Lasers in Medicine 3(4), 295 (2014).

[9] Zhang, A., and Wang, R. K., "Feature space optical coherence tomography based micro-angiography," Biomedical Optics Express 6(5), 1919 (2015).

[10] Matveev, L. A., Zaitsev, V. Y., Gelikonov, G. V., Matveyev, A. L., Moiseev, A. A., Ksenofontov, S. Y., Gelikonov, V. M., Sirotkina, M. A., Gladkova, N. D., Demidov, V., and Vitkin, A., "Hybrid M-mode-like OCT imaging of three-dimensional microvasculature in vivo using reference-free processing of complex valued B-scans," Optics Letters 40(7), 1472 (2015).

[11] Matveev, L. A., Zaitsev, V. Y., Gelikonov, G. V., Matveyev, A. L., Moiseev, A. A., Ksenofontov, S. Y., Gelikonov, V. M., Demidov, V., and Vitkin, A., "Scan-pattern and signal processing for microvasculature visualization with complex SD-OCT: tissue-motion artifacts robustness and decorrelation time-blood vessel characteristics," SPIE Proceedings 9448, 94481M (2015).